HONG SH DUBOW J 00/00/0000
MONITORING IN SITU RETORTING PROCESSES OF OIL SHALE BY REFLECTED AND TRANSMITTED ELECTROMAGN

Reference #

Data Inventory Sheet

1. Commodity OS
2. Author Hong, SH + A. DuBow
3. Title (or description)
   Monitoring in situ retorting processes of O shale by reflected + transmitted electromagnetic waves
4. Date ? 22 pp.
5. Reference
   ?
6. Source CSU, Dept. of Electrical Engr.
   Letc funded
7. Location of Data
   Duvall's loft file 224 dr. 1 (S. Wall)
8. Form of Data
9. Type of Work
10. Description of Work
11. Types of Data
12. Quantity of Data
13. Quality of Data
14. Priority

Ref OK

MONITORING IN SITU RETORTING PROCESSES OF OIL SHALE BY REFLECTED AND TRANSMITTED ELECTROMAGNETIC WAVES*

by

S. H. Hong and J. B. DuBow
Department of Electrical Engineering
Colorado State University
Fort Collins, Colorado 80523

Abstract

A theoretical model for an in situ oil shale retort with three distinct zones surrounded by the wall of oil shale deposits, the overburden and underburden, is considered to study monitoring the progression of retorting processes by means of the electromagnetic wave propagation. The overall power reflection and transmission coefficients for both transverse electric and transverse magnetic waves are obtained as a function of position of a combustion zone in the retort based upon the assumption of straight-line propagation of monocromatic plane waves through layered lossy dielectric media. The behavior of each power coefficient is discussed as a function of burn front positions in terms of frequencies. As a result of moderate power signal of each coefficient to detect, and the one-to-one correspondence between each power coefficient and burn front position at typical conditions, the feasibility of using low radio-frequency waves to monitor relatively large scale of in situ retorting process has been established.

*Supported by U.S. ERDA.

INTRODUCTION

Electromagnetic methods by the wave propagation in the rocks have the great practical potential in a wide variety of applications to the geological remote probing for processing and prospecting of underground resources.[1,2] Electromagnetic waves might be used to monitor the in situ retorting process of oil shale, which is an ideal technique for shale oil extraction due to lower recovery costs, a lesser environmental impact, and a much larger resource suitable for development in contrast to conventional mining and aboveground processing systems.[3]

For processing of oil shale in its existing formation, it is necessary to fracture the raw oil shale with little permeability deposited between an overburden and an underburden in order to create an in situ retort consisting of a underground chimney with broken oil shale. The increasing void volume and shale surface area allow adequate flow paths for gas and oil, and rapid reaction rate for in situ retorting. In a forward combustion process, the combustion flame initiated at the top of the retort chimney and sustained by an injected recycle gas stream advances slowly downward in the direction of gas stream through rubblied oil shale to a production well located at the bottom of the retort. On the other hand, the flame is ignited at the production well and moves upward against the oncoming gas stream in a reverse combustion process. The oil and gas yields produced by the pyrolysis of organic matter in oil shale are substantially recovered in the production well.[4] Consequently, three distinct areas are formed in the retort chimney, i.e., burned-out zone, combustion zone with relatively thin thickness, and cool zone with untreated rubblized oil shale. All these regions are physically disturbed from the initial state of raw shale as a result of void volume generated by fracturing and thermal transformation of oil shale occurred by the heat during retorting process. The electrical properties of oil shale in the retort chimney are therefore characterized by the discontinuities of the dielectric constant, conductivity, and magnetic permeability in three zones.

From the techrical aspects of in situ retorting process, the propagation of combustion front within retort chimney should be monitored and controlled for the proper operation. The efficient method of monitoring the movement of burn front would be through the electromagnetic instrumentation, of which design and installation utilize the propagation characteristics of electromagnetic waves from electrical discontinuities of three zones in the retort chimney together with the overburden and underburden. To date, however, no simple electromagnetic scheme appears to predict the behavior of operating procedures of in situ process for oil shale. The development of electromagnetic techniques for in situ processing requires a knowledge of electrical properties of oil shale. For this purpose, some limited data for electrical properties of oil shale have been measured in the author's laboratory.[5,6] An ability of electromagnetic systems to monitor the in situ coal gasification process has been investigated by a geometrical optics formulation.[7,8] At present, due to the absence of theoretical work on electromagnetic methods for oil shale the idea of using electromagnetic waves for in situ oil shale retorting has not been adequately tested or demonstrated.

The primary purpose of this investigation is to theoretically model the monitoring system for in situ retorting of oil shale. The model involves transmitting electromagnetic waves from the atmosphere through the entire length of in situ retort under the earth's surface. The remote probing can then be performed either at the surface or in a single drill hole by measuring a reflection or transmission power. The behavior of electromagnetic signal is a function of vertical positions of the combustion zone since the electrical discontinuities within the retort varies as the burn front moves. This investigation is concerned with an attempt to find the position and velocity of combustion zone and to determine the transmitting frequency range over which the electromagnetic technique might be applicable. The usefulness of the electromagnetic monitoring model for oil shale retorting process is analyzed based upon the assumption of straight-line propagation of linearily-polarized plane waves through layered lossy dielectric media.[9,10]

DESCRIPTION OF MODEL

As shown in Fig. 1, an in situ retort with burned-out, combustion, and cool zones consists of a rubblized oil shale chimney surrounded by a raw oil shale formation, an overburden and an underburden. A Cartesian coordinate system is introduced, with the x and y axes parallel to each layered region and the z axis normal to it. Each layered underground region along axial direction is assumed to be a homogeneous lossy dielectric medium with discontinuities occurring at interfaces, $z = -z_n$, $n = 0, 1, \ldots, 4$. Each region is then specified by a complex dielectric constant, $\varepsilon_n \equiv \varepsilon_n' - i\varepsilon_n''$ where a real part ε_n' is associated with an ability of the dielectric to store the electric energy, and an imaginary part ε_n'' is the loss factor associated with the power lost involving the conductivity of the medium. Since the magnetic permeabilities μ_n of oil shales and rocks are nearly equal to μ_o of free space, it is assumed that the underground media to be considered are magnetically homogeneous.[11] But, it is convenient to retain μ_n in order to obtain symmetrical expressions with respect to ε_n. The combustion zone extending over a relatively short distance $z_3 - z_2$ in the axial direction is moving downward (upward) with velocity $\vec{v}$ for the forward (reverse) process. The burning rate along the axial direction is assumed to be uniform so that the boundaries separating layered regions of the retort are planar.

A transverse electric (TE) or transverse magnetic (TM) plane wave is incident upon the air/overburden interface from the atmosphere. The incident wave is normal to the air/overburden discontinuity at $z = -z_o = 0$ parallel to other discontinuities at $z = -z_n$, $n = 1, \ldots, 4$. Then, the formulas for straight-line propagation adequately describe the dominant propagation mechanism between the transmitter and receiver located along the z axis. The pillar wall of the retort does not affect electromagnetic fields since the effects of refraction at the discontinuities and reflection from the raw shale wall are not considered. For a constant transmitter power, one can monitor the behavior of the signal level for reflected or tansmitted wave in the receiver as the combustion zone advances. The behavior of the signal for an overall power reflection coefficient $\overline{R}$ from the earth's surface $z = 0$ or an overall power transmission coefficient $\overline{T}$ at the bottom of the retort $z = -z_4$, is a function of moving burn front position $z = -z_3$ for the forward progress. The inversion of $\overline{R}(z_3)$ or $\overline{T}(z_3)$ gives the location of burn front $-z_3$, and the time variation of z_3 yields the speed of progression v.

OVERALL POWER COEFFICIENTS FOR TE AND TM WAVES

Consider electromagnetic fields for a TE plane monocromatic wave of angular frequency ω incident from free space,

$$\vec{E}_o(\vec{r},t) = \vec{A}_o e^{i\omega t - i\vec{k}_o \cdot \vec{r}},$$
$$\vec{H}_o(\vec{r},t) = (\omega \mu_o)^{-1} \vec{k}_o \times \vec{E}_o. \tag{1}$$

$|\vec{k}_o| = \omega(\mu_o \varepsilon_o)^{\frac{1}{2}}$ is the propagation constant in free space. The amplitude $\vec{A}_o$ is determined by the power of incident wave from the transmitter, i.e., is a known quantity. The mathematical expressions for a TM excitation can be obtained by duality with the replacements $\vec{E} \rightarrow \vec{H}$, $\vec{H} \rightarrow -\vec{E}$. and $\varepsilon \leftrightarrow \mu$, in view of Maxwell's equations:

$$\nabla \times \vec{E} = -i\omega\mu \vec{H}, \qquad \nabla \cdot \varepsilon \vec{E} = 0,$$
$$\nabla \times \vec{H} = i\omega\varepsilon \vec{E}, \qquad \nabla \cdot \mu \vec{H} = 0. \tag{2}$$

The spatial-dependent solutions for electromagnetic fields in each layered region ($n = 0,1,\ldots,5$) are written as the sum of waves transmitted downward in each medium and reflected upward at each discontinuity:

for TE waves,

$$E_{ny}(z) = A_n^+ e^{+ik_n z} + B_n^+ e^{-ik_n z},$$
$$H_{nx}(z) = Z_n^{-1} (A_n^+ e^{+ik_n z} - B_n^+ e^{-ik_n z}), \tag{3}$$

for TM waves,

$$H_{ny}(z) = A_n^- e^{+ik_n z} + B_n^- e^{-ik_n z},$$
$$E_{nx}(z) = -Z_n (A_n^- e^{+ik_n z} - B_n^- e^{-ik_n z}). \tag{4}$$

The characteristic wave impedence of a dielectric medium n is defined as

$$Z_n \equiv (\mu_n / \varepsilon_n)^{\frac{1}{2}}. \tag{5}$$

The complex propagation constant k_n is given by

$$k_n = \omega(\mu_n \varepsilon_n)^{\frac{1}{2}} = \left[\omega^2 \mu_n \varepsilon_n'(1-i \tan \delta_n)\right]^{\frac{1}{2}}, \tag{6}$$

$\tan \delta_n$ is referred to as the loss tangent of the layered medium n,

$$\tan \delta_n \equiv \varepsilon_n'' / \varepsilon_n' = \sigma_n / \omega \varepsilon_n' \tag{7}$$

where σ_n is a conductivity of n. For n = 5, $B_n^{\pm} = 0$ since there is no reflection waves in this region.

The wave amplitudes $A_n^{\pm}$ and $B_n^{\pm}$ are determined by boundary conditions for $\vec{E}$ and $\vec{H}$ at $z = -z_n$. Owing to the negligible speed of combustion zone (~2 m/day) compared with the speed of electromagnetic waves (3×10^8 m/sec), the Doppler shift in frequency and the moving effect of burning interfaces on boundary conditions can be neglected. Hence, the boundary conditions at $z = -z_n$ requires that tangential components of $\vec{E}$ and $\vec{H}$ be continuous across discontinuities, i.e., for TE waves,

$$E_{ny}(-z_n) = E_{(n+1)y}(-z_n), \qquad H_{nx}(-z_n) = H_{(n+1)x}(-z_n), \tag{8}$$

and for TM waves,

$$H_{ny}(-z_n) = H_{(n+1)y}(-z_n), \qquad E_{nx}(-z_n) = E_{(n+1)x}(-z_n). \tag{9}$$

Let a reflection coefficient R_n and a dimensionless wave impedance η_n in each region n defined for both TE(+sign) and TM(-sign) waves as

$$R_n^{\pm}(z) \equiv (B_n^{\pm}/A_n^{\pm})\, e^{-i2k_n z}, \tag{10}$$

and

$$\eta_n^{+}(z) \equiv \frac{Z_n}{E_{ny}(z)/H_{nx}(z)} = \frac{1 - R_n^{+}(z)}{1 + R_n^{+}(z)},$$
$$\eta_n^{-}(z) \equiv -\frac{E_{nx}(z)/H_{ny}(z)}{Z_n} = \frac{1 - R_n^{-}(z)}{1 + R_n^{-}(z)}. \tag{11}$$

Then, the application of boundary conditions (8) and (9) into Eqs. (3) and (4), respectively, using the expressions of Eqs. (10) and (11) yields

$$\frac{B_n^{\pm}}{A_n^{\pm}} = \frac{1 - \eta_n^{\pm}}{1 + \eta_n^{\pm}} e^{-i2k_n z_n}, \qquad n = 0,1,\ldots,4, \tag{12}$$

where

$$\eta_n^{\pm} \equiv \eta_n^{\pm}(-z_n) = \left(\frac{Z_n}{Z_{n+1}}\right) \frac{\eta_{n+1}^{\pm} + i \tan\left[k_{n+1}(z_{n+1}-z_n)\right]}{1 + i\,\eta_{n+1}^{\pm} \tan\left[k_{n+1}(z_{n+1}-z_n)\right]} \quad \text{for } n=0,1,2,3,$$

$$\eta_4^{\pm} = \eta_4^{\pm}(-z_4) = (Z_4/Z_5)^{\pm 1}. \tag{13}$$

Hence, the overall reflection coefficients become

$$R^{\pm} = R_o^{\pm}(-z_o=0) = \frac{1 - \eta_o^{\pm}}{1 + \eta_o^{\pm}} \tag{14}$$

where $\eta_o^{\pm}$ are determined by successive calculations of Eqs. (13). The overall transmission coefficients $T^{\pm}$ are determined in a similar manner by application of boundary conditions for E_{ny} and H_{ny}, respectively:

$$T^{\pm} \equiv A_5^{\pm} e^{-ik_5 z_4} / A_o^{\pm} e^{-ik_o z_o}$$

$$= 2/(1+\eta_o^{\pm}) \prod_{n=1}^{4} \left\{1 + i\,\eta_n^{\pm} \tan\left[k_n(z_n - z_{n-1})\right]\right\}. \tag{15}$$

It is noted that the results for TM waves can be obtained from those of TE waves by the exchange of ε_n and μ_n, and vice versa. It can then be shown the following relations between TE and TM waves,

$$\eta_n^{+} = 1/\eta_n^{-}, \qquad R^{+} = -R^{-}, \qquad T^{+} = (Z_5/Z_o)T^{-}. \tag{16}$$

The power reflection or transmission coefficient which gives the ratio of a reflected or transmitted intensity at the receiver to an incident intensity at the transmitter, respectively, for the measurement in the experiment, is determined by real parts of the complex Poynting vectors $\frac{1}{2} Re(\vec{E} \times \vec{H}^*)$, i.e.,

$$\overline{R}^{\pm} = |R^{\pm}|^2, \tag{17}$$

$$\overline{T}^{\pm} = \frac{Re(Z_5^{\mp 1})}{Re(Z_0^{\mp 1})} |T^{\pm}|^2. \tag{18}$$

The overall power absorption coefficients $\overline{A}^{\pm}$ through underground lossy media are simply given by the relation,

$$\overline{R}^{\pm} + \overline{T}^{\pm} + \overline{A}^{\pm} = 1. \tag{19}$$

It is remarkable that each power coefficient has the same value for TE and TM waves in view of Eqs. (16)-(19), i.e.,

$$\overline{R}^{+} = \overline{R}^{-}, \qquad \overline{T}^{+} = \overline{T}^{-}, \qquad \overline{A}^{+} = \overline{A}^{-}. \tag{20}$$

DISCUSSION OF NUMERICAL ILLUSTRATIONS

For the numerical evaluation of power coefficients for TE and TM waves given by Eqs. (17)-(19), consider a typical retort chimney which has a height z_4-z_1 of 100 m and a combustion zone with a thickness z_3-z_2 of 2 m. The assumed retort chimney extending laterally over a comparable distance with its height is thought to be located under the overburden with a thickness z_1-z_0 of 50 m. The dielectric constant ε_n' and the loss tangent tan δ_n are treated as the basic electrical parameters of each layered lossy medium, which are functions of frequency $\omega/2\pi$ of electromagnetic waves. Typical data showing the dependence of electrical parameters on the frequency are listed in Table 1 for each layered lossy media.[5,6,11]

Figs. 2-4 show the behavior of power coefficients $\overline{R}^{\pm}$, $\overline{T}^{\pm}$, and $\overline{A}^{\pm}$ as a function of burn front position z_3-z_1 for frequencies $\omega/2\pi = 10^4, 10^5, 10^6$ Hz in the forward combustion process. In Figs. 5-7, these coefficients are represented versus burn front position z_2-z_1 in the reverse combustion process. As the burned-out zone with relatively high conductivity is increased at the expence of the cool zone with the smaller conductivity, the power absorption coefficients are increased while the power transmission coefficients are decreased in both forward and reverse processes. This is due to the larger attenuation of electromagnetic fields as they travel greater distances in the higher lossy medium of the burned-out zone. High-frequency waves might not therefore be employed to study monitoring progression of in situ retort process in great depths under the ground. At low frequencies, all power coefficients vary nearly linear so that the one-to-one correspondence between each power coefficient and burn front position appears. As the frequency is increased, reflection and absorption coefficients start to reveal the oscillatory behavior.

It is concluded that the over-simplified monitoring model presented describes qualitatively well the physics of the actual field situation for in situ retorting processes. It is desirable to use low radio frequencies up to 10^5 Hz for monitoring the progression of retorting processes because of moderate powers of reflection and transmission coefficients to detect, and the one-to-one relationship mentioned above. Although reflection coefficients are not so sensitive to changes in burn front positions as transmission coefficients, the radio wave method of the measurement of reflected power is more suitable for monitoring the in situ process where it is accessible from one side only on the ground without drill holes.

REFERENCES

1. G.V. Keller and F.C. Frischknecht, Electrical Methods in Geophysical Prospecting(Pergamon, New York, 1966).

2. J.R. Wait, Electromagnetic Probing in Geophysics(Golem, Boulder, 1971).

3. T.F. Yen, Science and Technology of Oil Shale(Ann Arbor Science, Ann Arbor, 1976).

4. H.E. Wilhelm, J.B. DuBow, and S.H. Hong, J. Appl. Phys. 49, 5768 (1978).

5. K. Rajeshwar, R.N. Nottenburg, and J.B. DuBow, Thermochim. Acta 26, 1 (1978).

6. K. Rajeshwar, R.N. Nottenburg, J.B. DuBow, and R. Rosenvold, Thermochim. Acta 27, 357 (1978).

7. J.J. Holmes and C.A. Balanis, Radio Sci. 12, 33 (1977).

8. D.T. Davis and R.J. Lytle, Lawrence Livermore Laboratory Report UCRL-52325 (1977).

9. L.M. Brekhovskikh, Waves in Layered Media(Academic, New York, 1960).

10. J.R. Wait, Electromagnetic Waves in Stratified Media(Pergamon, New York, 1970).

11. E.I. Parkhomenko, Electrical Properties of Rocks(Plenum, New York, 1967).

TABLE 1. Relative dielectric constant $\varepsilon'_n/\varepsilon_o$ and loss tan δ_n of each layered lossy region n as a function of frequency $\omega/2\pi$.

$\omega/2\pi$	Region n	$\varepsilon'_n/\varepsilon_o$	tan δ_n
10^4 Hz	1, 5	17	0.6
	2	11	4.5
	3	9	6.0
	4	15	0.5
10^5 Hz	1, 5	16	0.2
	2	7	1.5
	3	6	3.0
	4	9	0.15
10^6 Hz	1, 5	15	0.16
	2	4	1.0
	3	3	1.5
	4	5	0.1

FIGURE CAPTIONS

FIG. 1. An in situ oil shale retort for a forward combustion process. For a reverse combustion process, burned-out and cool zones are interchanged each other, and the velocity $\vec{v}$ is reversed.

FIG. 2. Power coefficients($\bar{R}^{\pm}$, $\bar{T}^{\pm}$, $\bar{A}^{\pm}$) vs. burn front position z_3-z_1 for 10^4 Hz in forward combustion process.

FIG. 3. Power coefficients($\bar{R}^{\pm}$, $\bar{T}^{\pm}$, $\bar{A}^{\pm}$) vs. burn front position z_3-z_1 for 10^5 Hz in forward combustion process.

FIG. 4. Power coefficients($\bar{R}^{\pm}$, $\bar{T}^{\pm}$, $\bar{A}^{\pm}$) vs. burn front position z_3-z_1 for 10^6 Hz in forward combustion process.

FIG. 5. Power coefficients($\bar{R}^{\pm}$, $\bar{T}^{\pm}$, $\bar{A}^{\pm}$) vs. burn front position z_2-z_1 for 10^4 Hz in reverse combustion process.

FIG. 6. Power coefficients($\bar{R}^{\pm}$, $\bar{T}^{\pm}$, $\bar{A}^{\pm}$) vs. burn front position z_2-z_1 for 10^5 Hz in reverse combustion process.

FIG. 7. Power coefficients($\bar{R}^{\pm}$, $\bar{T}^{\pm}$, $\bar{A}^{\pm}$) vs. burn front position z_2-z_1 for 10^6 Hz in reverse combustion process.

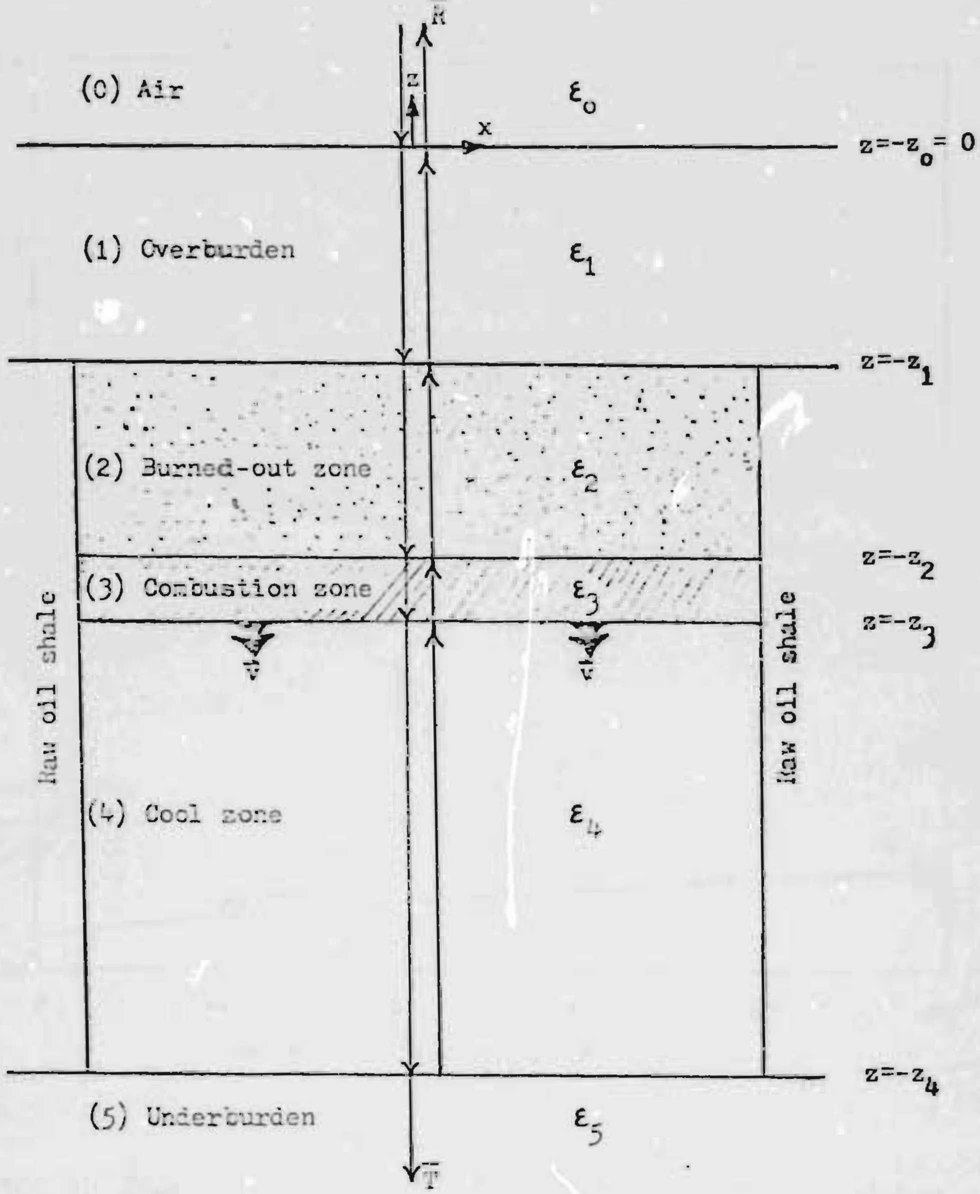

FIG. 1. An in situ oil shale retort for a forward combustion process. For a reverse combustion process, burned-out and cool zones are interchanged each other, and the velocity $\vec{v}$ is reversed.

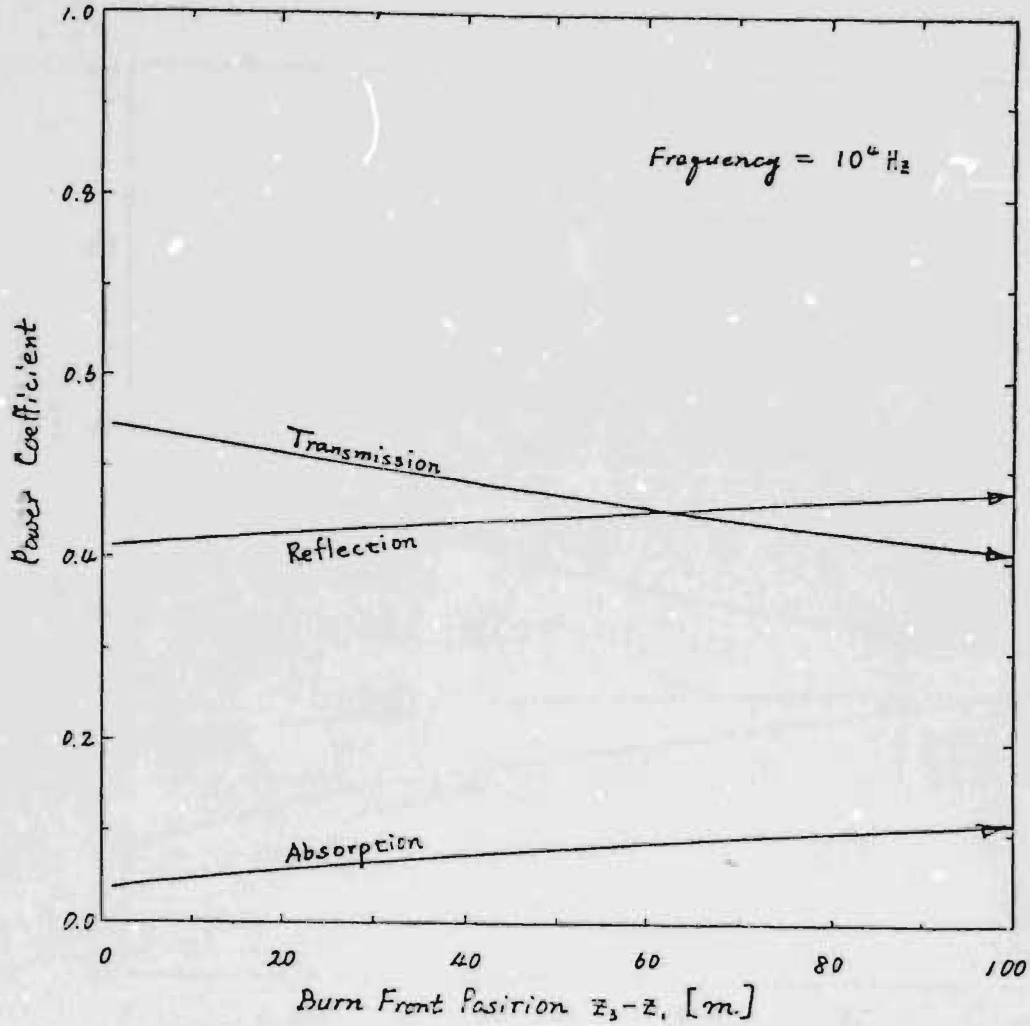

FIG. 2. Power coefficients($\bar{R}^{\pm}$, $\bar{T}^{\pm}$, $\bar{A}^{\pm}$) vs. burn front position z_3-z_1 for 10^4 Hz in forward combustion process.

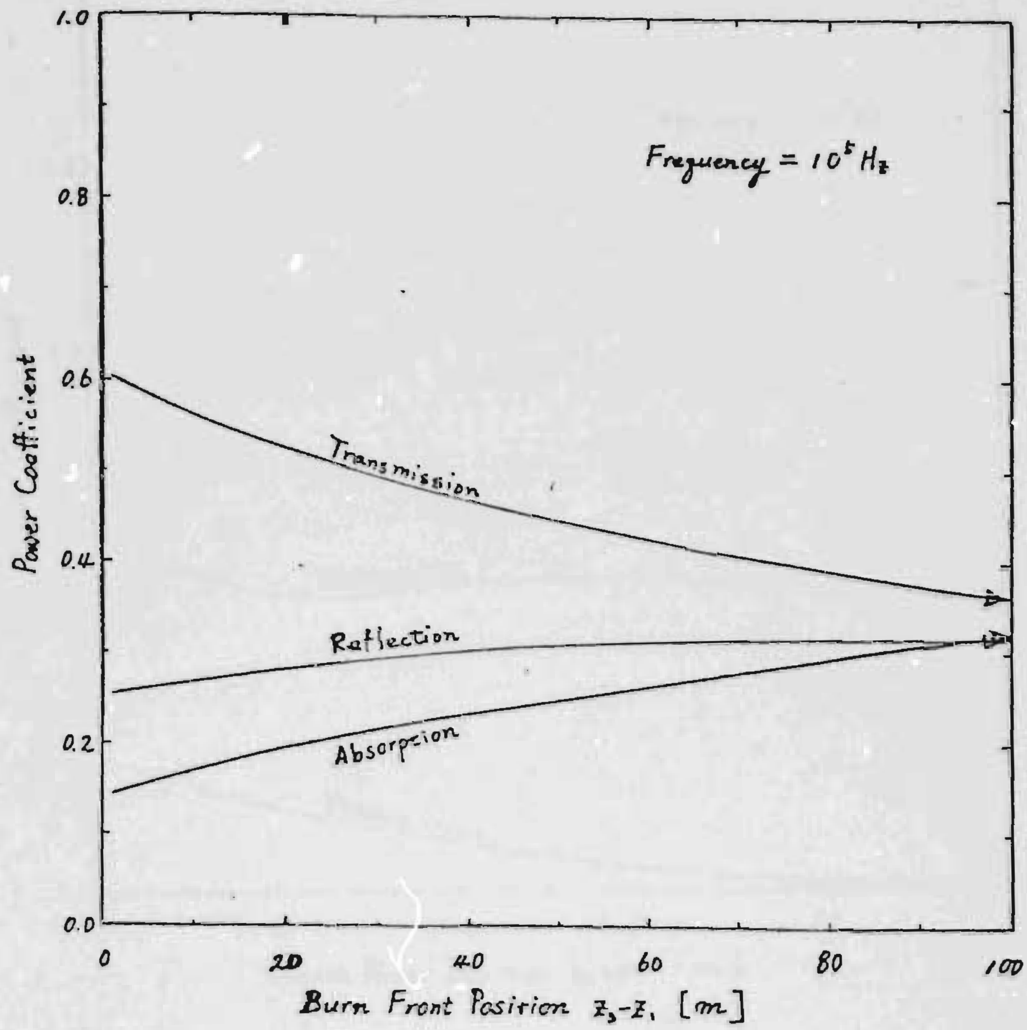

FIG. 3. Power coefficients($\bar{R}^{\pm}$, $\bar{T}^{\pm}$, $\bar{A}^{\pm}$) vs. burn front position z_3-z_1 for 10^5 Hz in forward combustion process.

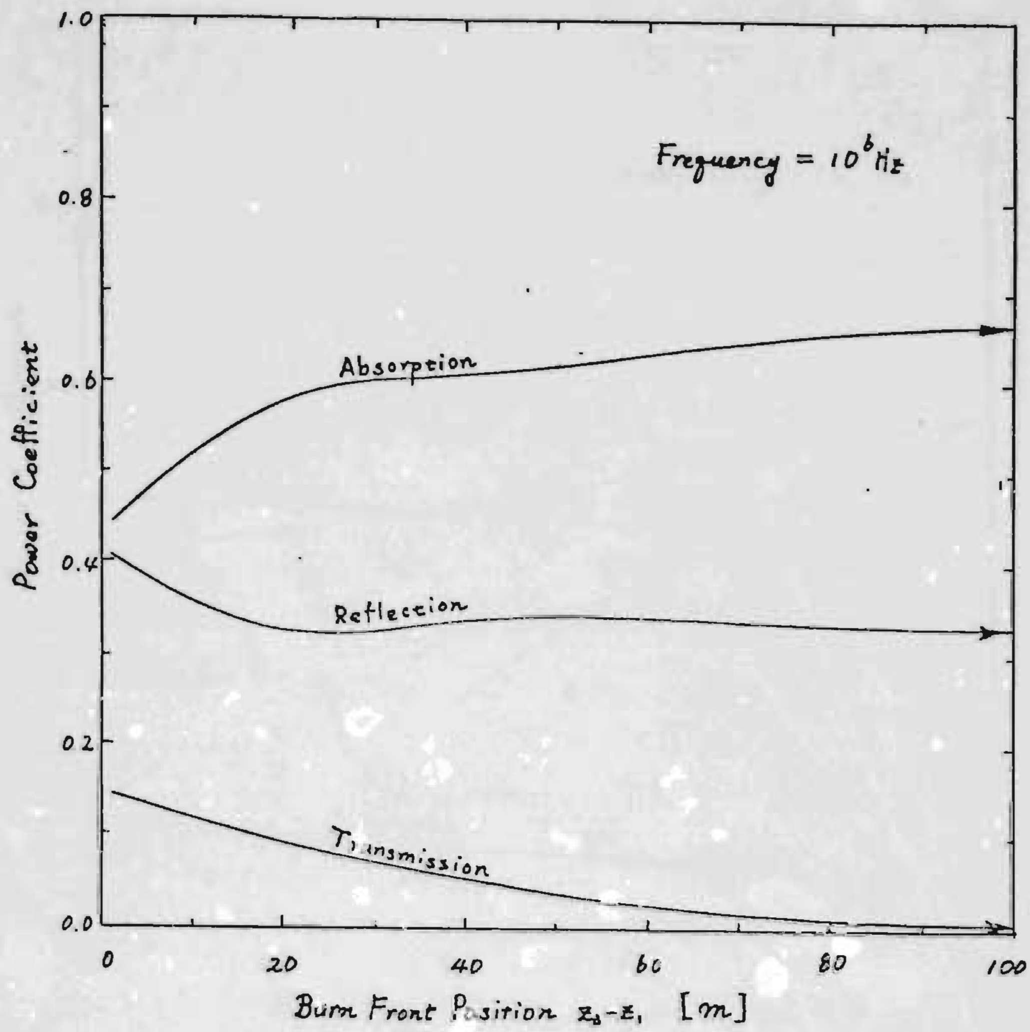

FIG. 4. Power coefficients($\bar{R}^{\pm}$, $\bar{T}^{\pm}$, $\bar{A}^{\pm}$) vs. burn front position z_3-z_1 for 10^6 Hz in forward combustion process.

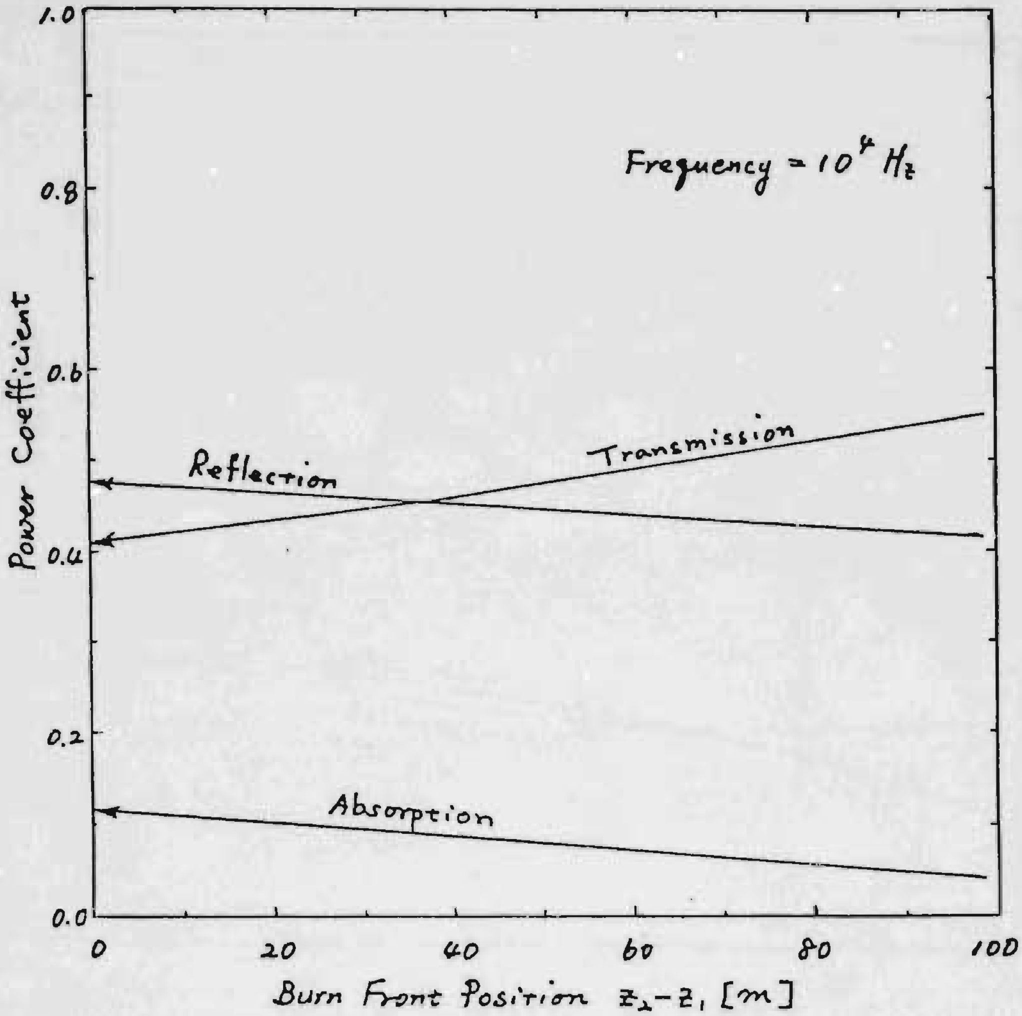

FIG. 5. Power coefficients($\overline{R}^{\pm}$, $\overline{T}^{\pm}$, $\overline{A}^{\pm}$) vs. burn front position z_2-z_1 for 10^4 Hz in reverse combustion process.

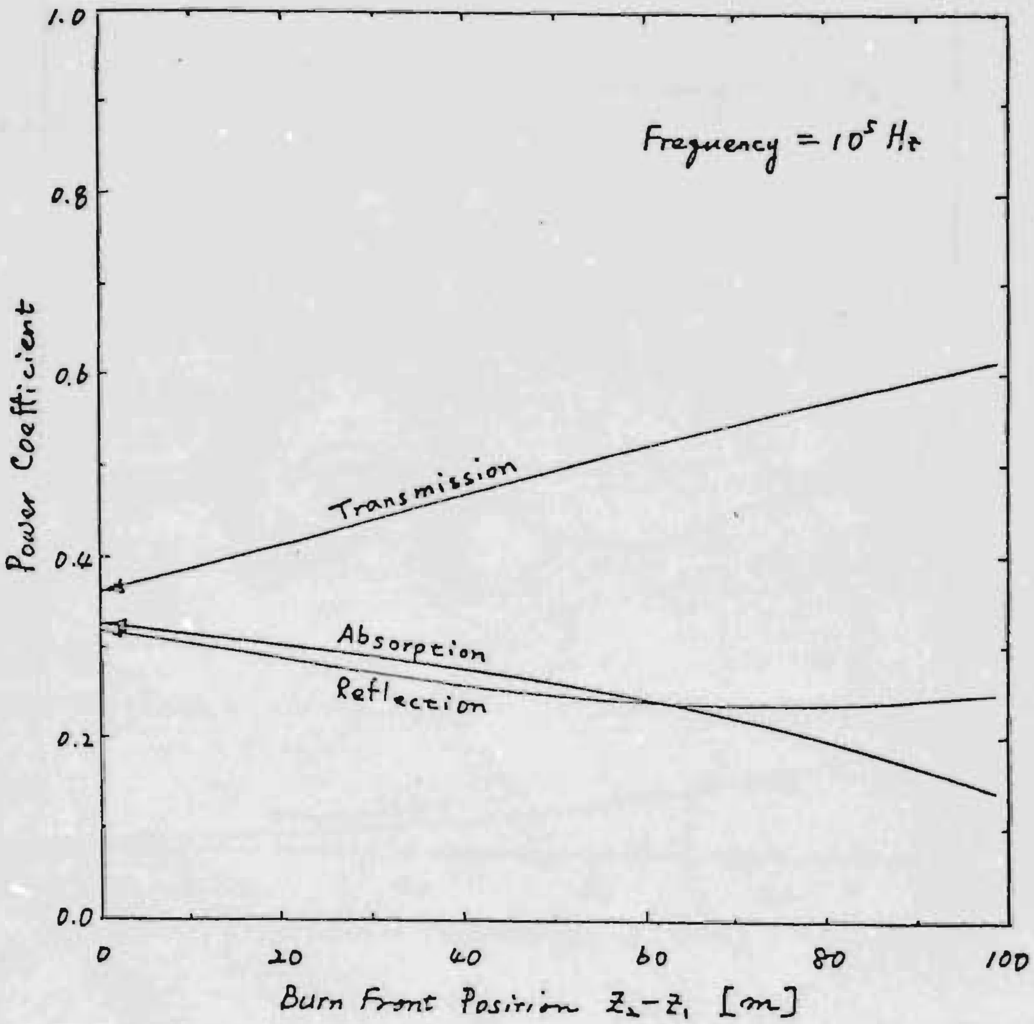

FIG. 6. Power coefficients($\bar{R}^{\pm}$, $\bar{T}^{\pm}$, $\bar{A}^{\pm}$) vs. burn front position z_2-z_1 for 10^5 Hz in reverse combustion process.

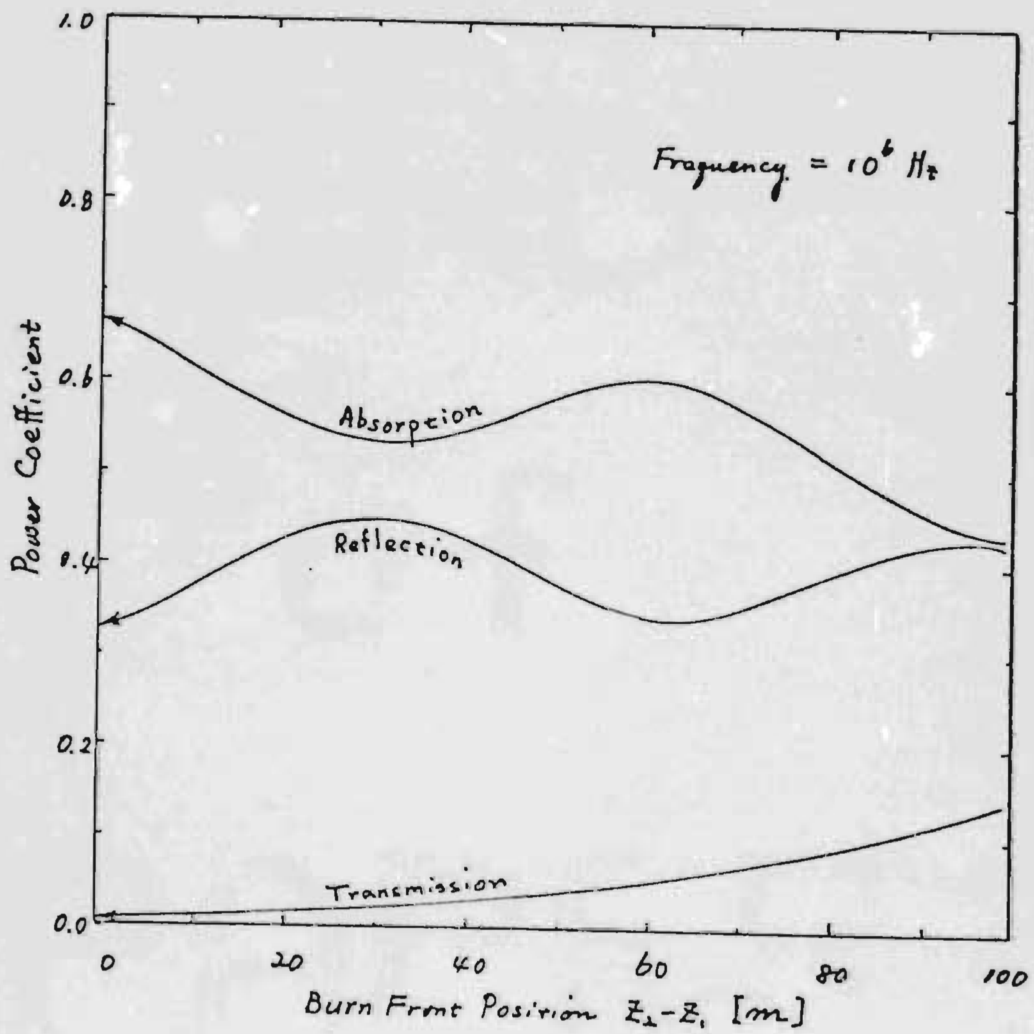

FIG. 7. Power coefficients($\overline{R}^{\pm}$, $\overline{T}^{\pm}$, $\overline{A}^{\pm}$) vs. burn front position z_2-z_1 for 10^6 Hz in reverse combustion process.

END

of

PAPER